Elsevier Editorial System(tm) for Remote Sensing of Environment
Manuscript Draft

Manuscript Number:

Title: Object-based mapping of the circumpolar taiga-tundra ecotone with MODIS tree cover

Article Type: Full length article

Keywords: taiga-tundra ecotone, MODIS, VCF, CAVM, CAPI

Corresponding Author: Mr. Ross F. Nelson,

Corresponding Author's Institution:

First Author: Kenneth J Ranson, PhD

Order of Authors: Kenneth J Ranson, PhD; Paul M Montesano, MS; Ross F. Nelson

Research Highlights:

Object-based mapping of the circumpolar taiga-tundra ecotone with MODIS tree cover

- MODIS Vegtation Continuous Fields data used to map northern transition.

- Circumpolar northern boreal transition from taiga to tundra mapped as an ecotone.

- Compare MODIS transition zone to 2 tree lines and Canadian Landsat % tree cover map:
  - Tree line 1 – CAVM: corresponds to 1- 23% MODIS % tree cover.
  - Tree line 2 – CAPI: corresponds to 1-12% MODIS % tree cover.
  - MODIS-Landsat differences of ~25% (worst case) demonstrated.

Object-based mapping of the circumpolar taiga-tundra ecotone with MODIS tree cover

K.J. Ranson[a], P.M. Montesano[b], and R. Nelson[a,c]

a. Code 614.4, Biospheric Sciences Branch, NASA/Goddard Space Flight Center, Greenbelt, Maryland 20771, USA
b. Sigma Space Corp., Lanham, MD,20706 USA
c. corresponding author: email: Ross.F.Nelson@nasa.gov, telephone: 1-301-614-6632

Abstract

The circumpolar taiga-tundra ecotone was delineated using an image segmentation based mapping approach with multi-annual MODIS Vegetation Continuous Fields (VCF) tree cover data. Circumpolar tree canopy cover (TCC) throughout the ecotone was derived by averaging MODIS VCF data from 2000 - 2005 and adjusting the averaged values using linear equations relating MODIS TCC to Quickbird-derived tree cover estimates. The adjustment helped mitigate VCF's overestimation of tree cover in lightly forested regions. An image segmentation grouped pixels representing similar tree cover into polygonal features (objects) that form the map of the transition zone. Each feature represents an area much larger than the 500m MODIS pixel to characterize the patterns of sparse forest patches on a regional scale. Comparisons of the adjusted average tree cover data were made with (1) two existing tree line definitions aggregated for each 1° longitudinal interval in North America and Eurasia and (2) Landsat-derived Canadian proportion of forest cover for Canada. The adjusted TCC from MODIS VCF shows, on average, <12% TCC for all but one regional zone at the intersection with independently delineated tree lines. Adjusted values track closely with Canadian proportion of forest cover data in areas of low tree cover. Those polygons near the boreal/tundra interface with either (1) mean adjusted TCC values between 5-20% , or (2) mean adjusted TCC values <5% but with a standard deviation > 5% were used to identify the ecotone.

Introduction

Earth's longest vegetation transition zone, the circumpolar taiga-tundra ecotone (TTE), stretches for more than 13,400 km around Arctic North America, Scandinavia, and Eurasia (Callaghan et al. 2002a). This ecotone is subjected to climate change (Serreze et al. 2000), and sensitive to climate change (Callaghan et al. 2002b). The shifting of local subarctic tree lines throughout the forest-tundra biome is linked to ecological processes at different spatiotemporal scales and will reflect future global climatic changes (Payette et al. 2001). Monitoring the dynamics of this forest-tundra boundary is critical for our understanding of the causes and consequences of the changes. High-latitude ecosystems, i.e. boreal forests and tundra, play an important role in the climate system (Bonan et al. 1995) and have been warming in recent decades (Chapin et al. 2005). Modeled effects of increased deciduous tree cover in high-latitudes show a positive feedback with temperature in the vegetated regions of the arctic (Swann et al. 2010). Improved understanding of the role of the forest-tundra boundary requires a concerted research effort to be conducted over a long enough time period to detect and quantify ecosystem feedbacks (Chapin et al. 2000). The objective of this study was to develop a framework for long term monitoring of the circumpolar tundra-taiga ecotone using satellite data. We accomplish this by preparing a validated map of MODIS percent forest cover for the entire ecotone with repeatable methods. This goal is to provide a benchmark for future studies of the tundra-taiga ecotone. We accomplish this by preparing a validated map of MODIS percent forest cover for the entire ecotone using

procedures easily replicated by others. The results provide a benchmark for future studies of the tundra-taiga ecotone.

Background

The TTE is dynamic because it is very sensitive to human activity and climate change. For example, during the last 6000 years in northern Eurasia a general cooling trend of about 2-4^{o}C was associated with a 400 – 500km southward retreat of larch and birch forest stands (Callaghan et al. 2002b). In the past three decades global average surface air temperatures have risen by approximately 0.6^{o}C (Hansen et al. 2006) while temperatures in parts of the Northern Hemisphere have warmed by as much as 2^{o}C (Hansen et al. 1999). If it is assumed that growth and reproduction are controlled by temperature, a rapid advance of the tree line would be predicted (Grace et al. 2002). The northward movement of the TTE may result if climatic warming persists over centuries or millennia (Skre et al. 2002). Some studies predict that up to about one half of the tundra could be colonized by trees by 2100 (Callaghan et al. 2002b; Harding et al. 2001).

There is general agreement that temperature is important in determining the northern extent of the boreal forest. Widespread degradation of permafrost has been shown in numerous studies (Pavlov 1994; Osterkamp and Romanovsky 1996; Osterkamp and Jorgenson 2006; Jorgenson et al. 2006). Recent observations suggest that, in an indication of northern climate warming, shrubs and forests are expanding into the tundra (e.g., Kharuk et al. 1998, 2002; Esper and Schweingruber 2004; Tape et al. 2006; Blok et al. 2010) and experimental evidence shows that increased shrub cover in the tundra is a response to warming (Walker et al. 2006). In a case study conducted by Rees et al.

(2002) in a portion of the West Siberian plain (66.5^{o}N, 70.75^{o}E) from 1968 to 1997, seven of their 20 test sites showed colonization by advancing forests, one showed an inconclusive shift in the tree line and one test site, which was surrounded by water and wetlands, showed evidence of forest retreat. The remaining 11 sites showed no appreciable forest advance but four of these sites had developed denser forest cover. In the Polar Ural mountains crown closure of stands increased 4-5 times and the tree line boundary shifted 100-300 m into the tundra (Kharuk et al. 1998). Devi et al. (2008) estimate the past century's forest expansion in this region has led to an increase in biomass of 40-75 Mg/ha. These observations are consistent with those in northern Canada (Payette and Gagnon 1985) while transects through the forest-tundra in eastern Canada have shown no significant correlations in the short term (5-20 years) with climatic variables, but do reveal a rise in tree line (Gamache and Payette 2005). In the TTE in western, central and eastern Canada white spruce density increased without any significant displacements of the Arctic tree line over the past 100-150 years (Payette et al. 2001). Recently established trees near the forest limit at coastal sites east of Hudson Bay are associated with warmer conditions over the past 100 years (Laliberté and Payette 2008). However, from the 1970s – 1990s, a Landsat-based study of the TTE in two areas of northern Canada has also shown that the extent of the boreal forest in these areas remain stable (Masek 2001). It is important to note that the position of northern portion of the boreal forest is likely influenced by a range of conditions that vary by region (Callaghan et al. 2002a; Crawford and Jeffree 2007; Crawford 2005).

Recent work indicates increased Arctic vegetation growth with climate warming. Experiments have shown that a 1-3°C temperature warming can increase the height and

cover of deciduous shrubs in the tundra after two growing seasons (Walker et al. 2006). Analysis of shrub growth rings in northwestern Russian Arctic tundra has revealed field data that closely follows the patterns found in the greening signal of shrubs in the satellite record since the 1980s (Forbes et al. 2010). Results from the analysis of Landsat time series in Canada's forest-tundra interface suggests shrub replacement of bare ground and lichen cover (Olthof et al. 2008). Kharuk et al. (2005) studied the expansion of evergreen conifers into larch-dominated forest, noting the increase in tree-stand density and the spread of larch in the ecotone. However, the patterns of vegetation growth may not be consistent across the taiga-tundra transition (Bunn and Goetz 2006; Verbyla 2008) or may be interpreted differently depending on the scale of the analysis (Alcaraz-Segura et al. 2010). Furthermore, vegetation change may in many cases depend on site-specific characteristics, particularly where there is a direct effect from human activities (Crawford et al. 2003; Virtanen et al. 2002; Vlassova 2002; Toutoubalina and Rees 1999; Rees et al. 2002; Hagner and Rigina 1998).

The transition from taiga to tundra is characterized by a change in tree cover density. The TTE is not a distinct edge but a transition area where patches of tundra and forest are mixed. It is not easily defined and can be difficult to identify and quantify. Timoney et al. (1992) described the TTE in Canada in terms of the ratio forest to tundra identified on aerial photographs and Timoney (1995) highlights major differences in the ecotone from west to east. Across the circumpolar ecotone the abundance of trees has been used to identify vegetation patterns and monitor these patterns for shifts indicative of vegetation's response to human activities and climate changes. Rees et al. (2002) discuss identifying and monitoring the TTE in Russia using Landsat and Synthetic

Aperture Radar (SAR) data and the potential and limitations associated with satellite observation. Esper and Schweingruber (2004) suggest that there is a circumpolar trend of changes in treeline occurring where there are notable temperature changes and consistent monitoring methods are needed (Frey and Smith 2007). Spectral un-mixing methods (Sun et al. 2004) and multi-angular and –temporal data (Heiskanen and Kivinen 2008) have been used to characterize tree cover in the TTE. Stow et al. (2004) discuss multi-temporal remote sensing of land cover change applications in the Arctic, presenting case studies with a range of spatial resolutions and extents with durations spanning months to decades. These studies have shown that the climatically induced changes in vegetation cover and composition in the Arctic need to be monitored at different spatial scales. Ranson et al. (2004) examined the capabilities of remote sensing data for identifying the tundra-taiga transition zone in Ary-mas, Siberia by mapping the tree abundances. Their results showed that Landsat-7 ETM+ image and C-band SAR (RADARSAT) were adequate for mapping tree density in this area. They also demonstrated that lower resolution data such as MODIS can also be used to characterize the transition zone when adequate training data are available.

Image segmentation has been used with MODIS data (Tilton et al. 2006) and to delineate forest features and analyze forested areas at multiple scales (Pekkarinen 2002; van Aardt et al. 2006; Achard et al. 2009). Segmentations of high resolution digital aerial imagery were used to delineate vegetation (seagrass) percent cover (Lathrop et al. 2006). The purpose of this technique is to group pixels into meaningful image objects that represent landscape features. While groups of adjacent remote sensing pixels within a particular land cover category may be similar, they typically exhibit internal

heterogeneity. The segmentation process aims to minimize internal segment (image object) heterogeneity by accounting for both local image texture and the size of groups of pixels (Baatz and Schäpe 2000). Image segmentation procedures are useful for characterizing boundaries between ecological regions, where patches of vegetation of varying densities and gaps can signal a transition between land cover types. McMahon et al. (2004) suggest that research on ecological regions should consider the hierarchical relationship of landscape elements. The mean and variance associated with individual image objects, coupled with the hierarchical relationship of objects and sub-objects can be used to quantify changes in vegetation patches and gaps across a geographic gradient. Furthermore, the segmentation process can facilitate remote sensing data fusion, by incorporating information from multiple datasets on a per-segment basis.

Methods

MODIS data acquisition and processing

Figure 1 is a composite Terra MODIS image of the northern hemisphere above 50^{o} latitude. This image represents the geographic scope and diversity in the vegetated boreal and arctic zones. Collection 4 (C4) MODIS VCF (MOD44b) data (USGS LPDAAC 2010) was acquired as 10° x 10° tiles for 6 years (2000 – 2005) for the 21 tiles shown in Figure 2. Tiles for continental North America spanned 50°N – 70°N and tiles for Eurasia spanned 60°N - 70°N. No C4 MODIS VCF data existed above 70°N, which accounts for the data gap in northern Siberia. The data tiles were mosaicked by year for both North America and Eurasia using ENVI 4.5 software (ENVI 2010). The 6 years of data were then combined to derive an average VCF dataset, where each pixel represented

167 the mean percent tree canopy cover value of the corresponding pixel across all of the 6
168 VCF yearly datasets. Finally, the Collection 5 MODIS land cover (MCD12Q1, IGBP
169 global vegetation classification scheme) was used to change those VCF pixels whose
170 corresponding land cover type was water to tree canopy cover values of zero. Two multi-
171 annual datasets, one for continental North America and one for Eurasia resulted from this
172 processing sequence, each maintaining the original sinusoidal projection of the 463.3m
173 (nominally 500m) pixel grid.

174 *VCF Adjustment*

175 Each continental multi-annual VCF mosaic was adjusted based on inversions of
176 the results of linear regressions, shown in Table 1, relating Quickbird-validated percent
177 tree cover to MODIS VCF percent tree canopy cover (Montesano et al. 2009). The
178 adjustments were applied for seven broad longitudinal zones representing very general
179 circumpolar regions on a pixel-by-pixel basis (Figure 3). A value of zero was assigned to
180 those pixels for which the adjustment equations resulted in negative values, while a value
181 of 100 was assigned to those pixels whose adjusted values exceeded 100 percent tree
182 canopy cover.

183 The tree canopy cover values for pixels of the adjusted multi-annual VCF mosaics
184 (VCF_{adj}) were examined within the taiga-tundra ecotone using two existing definitions of
185 tree line. Vector polylines, approximating the northern limit of trees, from both the
186 Circumpolar Arctic Vegetation Map (CAVM) (Walker et al. 2005) and the Circum-Arctic
187 Map of Permafrost and Ground-Ice Conditions (CAPI) (Heginbottom et al. 1993) were
188 decomposed into points at intervals of 463.3m (the size of a VCF pixel). These points
189 were used to sample corresponding VCF_{adj} pixels within one-degree longitudinal

intervals wherever the points overlay VCF_{adj} pixels. The VCF pixel-sized interval was used to avoid oversampling any single VCF pixel and risk skewing the mean VCF value in 1° interval. For each 1° interval, the mean VCF_{adj} value for all VCF_{adj} pixels intersecting the sampling points from both the CAVM and the CAPI treelines were used to determine the mean VCF_{adj} TCC at each treeline.

VCF_{adj} canopy cover was examined using data from the Canadian Forest Service of Natural Resources Canada. The dataset is a 1km derived product of the Earth Observation for Sustainable Development of Forests land cover products (EOSD) (Wulder et al. 2008). The value of each 1km grid cell represents the proportion of the cell occupied by the within-cell majority EOSD class. For the 2 broad circumpolar zones in which Canada lies, a zonal mean analysis was performed to compare proportion of forest values at 1 km (from EOSD) to mean TCC values from the VCF_{adj}. For each EOSD value from 0 – 100% forest cover, we computed the median VCF_{adj}.

VCF Segmentation

To further mitigate pixel-level noise in the relationship of VCF tree canopy cover and Quickbird-based validation of tree cover in the TTE, groups of similar adjacent pixels were aggregated in a segmentation process. The segmentation algorithm minimizes within-object variance by arranging groups of spectrally similar, adjacent pixels into polygon image objects, or segments. The segmentation was applied to both the North American and the Eurasia adjusted VCF mosaics. To facilitate processing, each mosaic was divided into tiles. North America was divided into three tiles, where the largest was 4600 pixels X 4800 pixels, while Eurasia was divided into 5 tiles, where the largest tile was 5000 pixels X 2400 pixels.

In addition to the VCF_{adj} raster dataset, vector layer datasets were used as masks to constrain the segmentations to land areas within previously delineated taiga and tundra biomes. The World Wildlife Fund's (WWF) Global Lakes and Wetlands Database (Lehner and Doll 2004) was used to apply a water mask to the VCF_{adj} mosaics for all water polygons labeled "lake", "river", or "reservoir" and complemented the water mask provided by the MODIS IGBP scheme. The WWF's Ecoregions (Olsen et al. 2001) vector dataset depicts global terrestrial ecoregions defined as large land units comprised of distinct species and natural communities. All ecoregions within the Boreal Forests/Taiga biome and the Tundra biome were included in the vector masking portion of the overall segmentation procedure.

The segmentation process involved two steps. The steps were arranged in a protocol to standardize the processing steps for each tile of the VCF_{adj}. The first step involved an initial coarse segmentation allowing the vector layers to mask portions of the VCF_{adj} land pixels that were outside the Boreal Forest/Taiga or Tundra biomes. Subsequent class assignments, masking and segmentations were performed based on the masks established in this first step. The second step, applied within the mask area, created image objects using consistent scale parameter and homogeneity criterion. The scale parameter guides the general size of the image objects, and depends on the homogenous nature of pixel values in an area (Baatz and Schäpe 2000). The more homogenous the data, the larger the objects tend to be. The goal of this segmentation procedure was to derive image objects that represented various tree cover (forest) patches, identifying gaps of little to no tree cover, and delineating landscape objects with varying tree cover densities. The homogeneity criterion is comprised of complementary

color and shape components. Eighty percent of the weight was given to the color component, which is associated with the digital value of the pixels. The shape component, which defines the textural homogeneity of the resulting image objects, received the remaining 20%.

Taiga-Tundra Ecotone Mapping

The mapping portion was accomplished by classifying image objects based on a specified range of image object values that represent the TTE. For each image object, mean and standard deviation were calculated and attributed. The mean and standard deviation values were derived from the VCF_{adj} pixels that make up the image object. Image objects, whose sizes ranged widely depending on the nature of local VCF_{adj} value homogeneity, were considered part of the TTE if they fit one of the following two criteria:

1. The mean VCF_{adj} value was 5% - 20%.
2. The mean VCF_{adj} value was < 5% and the standard deviation > 5%.

Values within the biomes "Boreal Forest/Taiga" and "Tundra" that did not meet these criteria were not considered part of the TTE. Image objects whose mean adjusted value and standard deviation were both less than 5% were considered outside the TTE and classified as tundra while image objects with a mean VCF_{adj} value greater than 20% were not considered part of the TTE, and classified as boreal forest.

Results

Examining the Adjusted VCF

258 The intersection of VCF_{adj} polygons with two representations of tree-line was
259 produced for the circumpolar ecotone below 70°N. The intersection of the datasets show
260 the correspondence of low VCF_{adj} %TCC values with tree-line in North America and
261 Eurasia compiled for each regional zone (Table 2). The regional zone means are an
262 aggregation of the 1° longitudinal means of the VCF_{adj} values at their intersection with
263 each tree-line. Adjusted values above 20% are reported for the Western Eurasia regional
264 zone (40°E – 60°E), while all other zones average less than 12% VCF_{adj} tree cover at
265 both tree-lines. Most of the regional zones have a mean %TCC less than 5 for at least
266 40% of their 1 degree intervals (5 of 6 of the zones at the CAVM tree line, 6 of 7 at the
267 CAP tree line). This is indicative of agreement among the tree line data and the VCF_{adj}
268 on areas of low %TCC.
269 Plots of mean VCF_{adj} values for each 1° longitudinal zone in North America
270 (Figure 4a) and Eurasia (Figure 4b), show the performance of the VCF_{adj} across the
271 circumpolar transition zone. In North America, particularly west of Hudson Bay, the
272 linear adjustments brought %TCC values to near zero in many longitudinal zones. In
273 Eurasia, VCF_{adj} values are more variable, and spikes in %TC are apparent between 55°E
274 and 80°E. There is a broad gap in Figure 4b between 88°E and 148°E where, for the
275 most part, the CAVM and CAPI tree-lines lie above 70°N, where C4 VCF data was not
276 available. An interruption of the intersection between the tree-lines and the VCF_{adj} also
277 occurs in North America at Hudson Bay.
278 We compared the VCF_{adj} to the EOSD-derived proportion of forest within a 1km
279 x 1km grid cell. The proportion of forest is a product aggregated from the 25m Landsat-
280 based EOSD land cover data for Canada (Wulder et al. 2008). The dataset was provided

281 in the Lambert Conformal Conic projection and was resampled to the sinusoidal
282 projection to match that of the VCF. It covers nearly 6.6 million sq. km., approximately
283 1.7 million of which lie in the Eastern Canada zone and 4.9 of which lie in the Western
284 Canada zone. The dataset accounts for nearly one third of the world's boreal forest, and
285 one tenth of the global forest cover. The median VCF_{adj} value associated with each
286 EOSD 1% bin was plotted for both of Canada's regional zones (Figure 5). Although the
287 VCF_{adj} values range from 0% - 100% for all EOSD bins, the median VCF_{adj} is within an
288 average of 5% TCC between EOSD bins 0-30 for both Eastern and Western Canada. The
289 low %TCC portion of the plot is of particular interest because the adjustment algorithms
290 applied to the VCF were designed for areas of low TCC.
291 The EOSD - VCF_{adj} comparison illustrated in Figure 5 is an approximation
292 because the two products are responding to two different definitions of forest. The
293 VCF_{adj} map reports a 500m pixel, whereas the EOSD map reports percent forest cover in
294 a $1km^2$ cell. The EOSD data reflects the proportion of the $1km^2$ cell occupied by the
295 plurality EOSD class, forest. Exclusion of areas of significant tree/forest cover is
296 possible, when extensive forest cover (e.g. 40%) is eclipsed within a cell by another more
297 dominant land cover comprising the remaining 60% of the cell. In such a case, this
298 particular cell would not be included in the proportion of forest cover product, and thus
299 would not have an effect on this comparison of the two datasets. However, tree cover not
300 reflected in the EOSD forest category can result in the VCF_{adj} showing higher %TCC
301 values than EOSD forest cover values.
302 *The Circumpolar Taiga-Tundra Ecotone Map*

303 The map delineates a global scale circumpolar taiga-tundra ecotone for the base
304 period 2000-2005. The map data is cast in the sinusoidal projection, matching the
305 original projection of the input VCF. In Eurasia, the map extends from 60°N – 70°N, and
306 in North America from 50°N – 70°N, excluding Baffin Island in north-eastern Canada
307 and the Aleutian Peninsula in south-western Alaska. Figure 6a shows the map of the
308 circumpolar TTE in a polar projection. Figures 6b-g show greater detail for each regional
309 zone. These regional maps highlight the variability of the ecotone between regions as
310 well as the patchy nature
311 The data exists in digital GIS format, as both raster GeoTiff files and vector
312 shapefiles. The vector shapefiles contain mean and standard deviation VCF_{adj} percent
313 tree canopy cover values for each ecotone polygon, as well as the area of each polygon in
314 square kilometers. The ecotone is delineated with two classes. Class 1 is comprised of
315 polygons of 5%-20% mean tree canopy cover. Polygons with less than 5% mean tree
316 canopy cover but with a standard deviation greater than 5% make up Class 2. The
317 minimum polygon size for 95% of the TTE objects is 2.5 sq. km., which corresponds to
318 the minimum mapping unit. Greater than 95% of the area mapped as ecotone is
319 comprised of polygons that are at least 20 sq. km. in size.
320 The ecotone, below 70°N, covers over 1.9 million sq. km., 64% of which is found
321 in North America. Table 3 summarizes the area of each ecotone class by regional zone as
322 well as the ratio of Class 1 to Class 2. Regional ecotone areas range widely from 49k –
323 322k sq. km. in Class 1 and from 33k-301k sq. km. in Class 2. This may be largely due
324 to the longitudinal extent of each zone. The ratio of Class 1 to Class 2 reported in Table
325 3 provides insight into the nature of the transition and may indicate the ability of MODIS

to identify taiga-tundra transition across a region using MODIS-level satellite monitoring. Class 2 shows where tree cover may occur at densities too low to be reliably detected by MODIS. Notice the high ratio value for Western / Central Canada, where the ecotone is compact and easily demarcated compared with the low value for Eastern and Western Eurasia where the ecotone is appears more disjoint.

Discussion

We use adjusted values of a continuous tree canopy cover values from the MODIS VCF to map the ecotone at the taiga-tundra interface. The adjustment algorithms applied to VCF tree canopy cover pixels were based on validation results for the circumpolar taiga-tundra ecotone. The adjustment decreases the overestimation of tree canopy cover in areas of low tree cover, such as the transition from closed canopy boreal forest to open tundra. The map was created by grouping homogenous, adjacent sets of pixels using image segmentation. Ecotone polygons based on the original 500m pixel data were divided into two classes according to internal mean tree canopy cover and variance. These classes are bounded by a maximum TCC of 20%. This upper bound is consistent with the definition of the lower limit of forest in Potapov et al. (2008), where global intact forest landscapes were mapped using VCF TCC above 20%. The purpose of the segmentation process was to reduce pixel-level scatter, and derive patches of low tree canopy cover. While patches of low VCF_{adj} TCC do not necessarily indicate an ecotone, their proximity to the boundary of the Boreal Forest/Taiga and Tundra biomes help define the collective meaning of groups of patches. These groups of patches illustrate the

complex regional variations in the transition from forest to tundra, and identify the circumpolar taiga-tundra ecotone for the 2000-2005 base period.

The circumpolar taiga-tundra ecotone map shows regional differences across both North America and Eurasia. In the Central Canada zone (west of Hudson Bay), the map depicts an ecotone that is relatively well defined and show a NW-SE orientation. In this zone, ecotone polygons coalesce revealing a visually identifiable, rapid NE-SW transition of patches of homogenous low tree canopy cover**.** The steep vegetation gradients of this portion of the ecotone, well documented in Timoney et al. (1992) and Payette et al. (2001), are due to elevation changes, parent material and fire history. Timoney et al (1992) indicate that changes in the width of the ecotone in Canada are also correlated with radiation, climate, and edaphic conditions. The ecotone east of Hudson Bay is more discontinuous, possibly due to trees' difficulty in reproducing after disturbances (Payette and Gagnon 1985, ACIA 2005). Other portions of the circumpolar ecotone, such as the Eastern Eurasia zone, reveal a more fragmented environment where the transition from closed canopy forest to open tundra at the regional scale may be driven by topographical influences.

The comparison of the two tree lines with the VCF_{adj} shows good agreement between two representations of the northern extent of tree cover. Since the MODIS-resolution map cannot delineate tree line, we acknowledge the inherent difficulty in comparing the CAVM and CAPI lines with polygons based on groups of 500m pixels. Our method of sampling the VCF_{adj} using points along each tree line spaced at a distances equal to the width of a MODIS pixel provided a good estimate of the performance of the VCF_{adj} at 1° longitudinal intervals. The low mean values in Canada

371 and the relatively higher values in Eurasia are not surprising. The Canadian ecotone is
372 more compact and thus easier to depict with a line. Sections of the ecotone that are more
373 fragmented are less likely to have an easily identifiable tree line. This, in part, may
374 account for some component of the spikes in mean VCF_{adj} value in the 1° zones in
375 Western Eurasia. However, the spikes may be due, in large part, to artifacts of the
376 adjustment. The linear adjustment algorithms were designed to reduce the
377 overestimations of tree canopy cover in areas of low TCC. Where the VCF did not
378 initially identify low tree cover, the VCF_{adj} will show increased %TCC values. This may
379 be occurring in some the longitudinal zones showing spikes in VCF_{adj} relationship with
380 tree line data. These areas should be considered for more local scale refinement.
381 Furthermore, latitude may not be the primary determinant constraining the ecotone
382 throughout the region. Geographic features such as river corridors traversing a north-
383 south gradient through the ecotone may account for significant variations in local tree
384 cover conditions.

385 Although the VCF maps tree canopy cover, there is evidence that the VCF TCC
386 product confuses trees with shrubs (Heiskanen 2008, Gessner et al. 2008, Montesano et
387 al. 2009). As the arctic warms, the increase in shrub cover that is correlated to a greening
388 signal, described by Forbes et al. (2010), may be inadvertently documented by the VCF.
389 The adjustment of the VCF addresses the confusion between shrub and tree cover greater
390 than 5m (Hansen et al. 2003), however some shrub/tree confusion most likely persists.

391 The C4 VCF data gap above 70°N presents a problem where the ecotone extends
392 above this latitude. There are several areas above 70°N where visual inspection of high-
393 resolution multispectral imagery reveals forested patches; northern Scandinavia and

394 Russia's Taimyr Peninsula and Yana River delta. Documenting these portions of the
395 ecotone is critical. We expect an updated VCF product in late 2010 that will include
396 processing of MODIS tiles above 70°N. We plan to update the ecotone map with those
397 datasets when they become available.

398 This TTE map can be a used in a number of ways. First, it can be included in
399 global models that require forest extent information for the high northern latitudes. The
400 map provides an explicit northern extent for the boreal forest/taiga. Second, when used
401 as a mask the map provides a means by which vegetation structural changes can be
402 monitored. Finally, it may be used as the multispectral component in data
403 integration/fusion studies examining vegetation structure such as height and biomass with
404 finer resolution radar and lidar data.

405

406 **Conclusions**

407 We mapped the circumpolar taiga-tundra ecotone using 500m MODIS VCF data
408 from 2000-2005 adjusted to improve tree canopy cover delineation in areas of low tree
409 cover. The map provides an estimation of the transition between boreal forest/taiga and
410 tundra and is a benchmark for subsequent monitoring. We mapped the ecotone from
411 50°N-70°N in North America and 60°N-70°N in Eurasia with polygons of VCF_{adj} tree
412 canopy cover below 20%. The internal composition of each polygon is characterized by
413 mean and variance values that explain the heterogeneity of the VCF_{adj} pixels that form
414 the polygon classes of tree cover. The first class, covering > 1.3 million sq. km.
415 represents 5-20% adjusted tree canopy cover. The second class, covering >0.6 million
416 sq. km. represents patches of adjusted tree canopy cover <5% with standard deviations

>5%. The minimum mapping unit is approximately 2.5 sq. km., which is the minimum size of 95% of the class 1 and 2 ecotone polygons. Groups of polygons reveal the variability of the ecotone across 7 regional zones. The consistent treatment of the entire circumpolar region facilitates comparisons between regions and use with other global datasets.

Acknowledgments

This work was supported by NASA's Earth Science Division as part of the International Polar Year program.

References

ACIA. (2005). Impacts of a Warming Arctic: Arctic Climate Impact Assessment. Cambridge University Press, Cambridge.

Achard, F., Beuchle, R., Bodart, C., Brink, A., Carboni, S., Eva, H., Mayaux, P., Rasi, R., Simonetti, D., & Stibig, H.J. (2009). Monitoring forest cover at global scale: the JCR approach, *Proceedings of the 33rd ISRSE conference*, 4 pp.

Alcaraz-Segura, D., Chuvieco, E., Epstein, H.E., Kasischke, E.S., & Trishchenko, A. (2010). Debating the greening vs. browning of the North American boreal forest: differences between satellite datasets. *Global Change Biology*, *16*, 760-770.

Baatz, M. & Schäpe, A. (2000). Multiresolution segmentation: an optimizing approach for high quality multi-scale image segmentation. In: Angewandte Geographisch Informationsverarbeitung, XII Strobl, J. and T. Blaschke, editors. Wichmann. Heidelberg. pp. 12–23.

Blok, D., Heijmans, M., Schaepman-Strub, G., Kononov, A.V., Maximov, T.C., & Berendse, F. (2010). Shrub expansion may reduce summer permafrost thaw in Siberian tundra. *Global Change Biology*, *16*, 1296-1305.

Bonan, G.B., Chapin III, F.S., & Thompson, S.L. (1995). Boreal forest and tundra ecosystems as components of the climate system. *Climate Change*. 29, 145-167.

Bunn, A.G., & Goetz, S.J. (2006). Trends in satellite-observed circumpolar photosynthetic activity from 1982 to 2003: The influence of seasonality, cover type, and vegetation density. *Earth Interactions*, *10*, 1-19.

Callaghan, T.V., Crawford, R.M.M., Eronen, M., Hofgaard, A., Payette, S., Rees, W.G., Skre, O., Sveinbjornsson, J., Vlassova, T.K., & Werkman, B.R. (2002a). The dynamics of the tundra-taiga boundary: An overview and suggested coordinated and integrated approach to research. *Ambio*, 3-5.

Callaghan, T.V., Werkman, B.R., & Crawford, R.M.M. (2002b). The tundra-taiga interface and its dynamics: Concepts and Applications. *Ambio*, 6-14.

Chapin III, F.S., McGuire, A.D., Randerson, J., Pielke Sr., R., Baldocchi, D., Hobbie, S.E., Roulet, N., Eugster, W., Kasischke, E., Rastetter, E.B., Zimov, S.A., & Running, S.W. (2000). Arctic and boreal ecosystmes of western North America as components of the climate system. *Global Change Biology*. 6(1), 211-223.

Chapin III, F. S., Sturm, M., Serreze, M. C., McFadden, J. P., Key, J. R., Lloyd, A. H., McGuire, A. D., Rupp, T. S., Lynch, A. H., Schimel, J. P., Beringer, J., Chapman, W. L., Epstein, H. E., Euskirchen, E. S., Hinzman, L. D., Jia, G., Ping, C. L., Tape, K. D., Thompson, C. D. C., Walker, D. A., and Welker, J. M. (2005). Role of land-surface changes in Arctic summer warming, Science, 310, 657–660.

Crawford, R.M.M. (2005). Trees by the sea: advantages and disadvantages of oceanic climates. Proceedings of the Royal Irish Academy, 105B, 129-139.

Crawford, R.M.M. & Jeffree, C.E. (2007). *Northern climates and woody plant distribution*. In "Arctic-alpine ecosystems and people in a changing environment" (ed. J.B. Orbaek, R Kallenborn, I Tombre, EN Hegseth, S Falk-Petersen, AH Hoel), pp. 85-104. Springer Verlag, Berlin ISBN- 10 3-540-48512-4 and ISBN-13 978-3-540-48512-4

Crawford, R.M.M., Jeffree, C.E., & Rees, W.G. (2003). Paludification and forest retreat in northern oceanic environments. *Annals of Botany*, 91(2), 213-226. doi:10.1093/aob/mcfl85

Devi, N., Hagedorn, F., Moiseev, P., Bugmann, H., Shiyatov, S., Mazepa, V. & Rigling, A. (2008). Expanding forests and changing growth forms of Siberian larch at the Polar Urals treeline during the 20th century (pages 1581–1591), Global Change Biology, 14(7), 1455–1702. DOI: 10.1111/j.1365-2486.2008.01583.x

Esper, J., & Schweingruber, F.H. (2004). Large-scale treeline changes recorded in Siberia. *Geophysical Research Letters, 31*, 1-5.

Forbes, B.C., Fauria, M.M., & Zetterberg, P. (2010). Russian Arctic warming and 'greening' are closely tracked by tundra shrub willows. *Global Change Biology, 16*, 1542-1554.

Frey, K. E., & Smith, L.C. (2007). How well do we know northern land cover? Comparison of four global vegetation and wetland products with a new ground-truth

database for west Siberia. *Global Biogeochemical Cycles*, 21, GB1016, doi:10.1029/2006GB002706.

Gamache, I. & Payette, S. (2005). Latitudinal response of subarctic tree lines to recent climate change in eastern Canada. *Journal of Biogeography*, 32, 849-862.

Gessner, U., Conrad, C, Hüttich, C., Keil, M., Schmidt, M., Schramm, M., & Dech, S. (2008). A multi-scale approach for retrieving proportional cover of life forms. IEEE International Geoscience and Remote Sensing Symposium, 700-703.

Grace, J., Berninger, F., & Nagy, L. (2002). Impacts of climate change on tree line. *Annals of Botany.* 90(4), 537-544.

Hagner, O., & Rigina, O. (1998). Detection of forest decline in Monchegorsk area. *Remote Sensing of Environment*, 63(1), 11-23.

Hansen, M. C., Defries, R., Townshend, J., Carroll, M., Dimiceli, C., & Sohlberg, R. (2003). Global percent tree cover at a spatial resolution of 500 meters: First results of the MODIS vegetation continuous fields algorithm. *Earth Interactions*, 7, 1-15.

Hansen, J., Ruedy, R., Glascoe, J., & Sato, M. (1999). GISS analysis of surface temperature change. *Journal of Geophysical Research*, 104, 30997-31022. doi:10.1029/1999JD900835

Hansen, J., Sato, M., Ruedy, R., Lo, K., Lea, D.W., & Medina-Elizade, M. (2006). Global temperature change. *Proceedings of the National Academy of Sciences*. 103 (39), 14288-14293.

Harding, R.J., Gryning, S.E., Halldin, S., & Lloyd, C.R. (2001). Progress in understanding of land surface/atmosphere exchanges at high latitudes. *Theoretical Applied Climatology.* 70, 5-18.

Heginbottom, J.A., J. Brown, E.S., Melnikov, & Ferrians, Jr., O.J. (1993). Circum-arctic map of permafrost and ground ice conditions, *Proceedings of the Sixth International Conference on Permafrost*, Wushan, Guangzhou, China: South China University Press, Vol. 2: 1132-1136. Revised December 1997. Boulder, CO: National Snow and Ice Data Center/World Data Center for Glaciology.

Heiskanen, J. (2008). Evaluation of global land cover data sets over the taiga–tundra transition zone in northernmost Finland. *International Journal of Remote Sensing*, 29(13), 3727−3751.

Heiskanen, J. & Kivinen, S. (2008). Assessment of multispectral, -temporal and –angular MODIS data for tree cover mapping in the tundra-taiga transition zone. *Remote Sensing of Environment*, 112, 2367-2380.

546 Jorgenson, M.T., Shur, Y.L., & Pullman, E.R. (2006). Abrupt increase in permafrost
547 degradation in Arctic Alaska. *Geophysical Research Letters.* 33, L02503.
548 doi:10.1029/2005GL024960.
549
550 Kharuk, V.I., Dvinskaya, M. L., Ranson, K. J., Im, S. T. (2005). Expansion of evergreen
551 conifers to the larch-dominated zone and climatic trends. *Russian Journal of Ecology,*
552 36(3), 164-170.
553
554 Kharuk, V. I., Ranson, K. J., Tret'yakova, V., & Shashkin, E. A. (2002). Reaction of the
555 larch dominated communities on climate trends. In L. E. Paques (Ed.), Proceedings of an
556 International Symposium "Improvement of Larch (Larix sp.) for better growth, stem form
557 and wood quality". France Gap, September 16–21 (pp. 289– 295). INRA.
558
559 Kharuk, V. I., Shiyatov, S. G., Naurzbaev, M. M., & Fedotova, E. V. (1998). Forest–
560 tundra ecotone response to climate change. In Severin Woxhott (Ed.), Proceeding of
561 IBFRA-98 (pp. 19– 23). Oslo, Norway: Oslo, Sept 21–23.
562
563 Laliberté, A.C., & Payette, S. (2008). Primary succession of subarctic vegetation and soil
564 on the fast-rising coast of eastern Hudson Bay, Canada. *Journal of Biogeography, 35,*
565 1989-1999.
566
567 Lathrop, R.G., Montesano, P., & Haag, S. (2006). A multi-scale segmentation approach
568 to mapping seagrass habitats using airborne digital camera imagery. *Photogrammetric*
569 *Engineering & Remote Sensing*, 72(6), 665-675.
570
571 Lehner, B., & Doll, P. (2004). Development and validation of a global database of lakes,
572 reservoirs and wetlands. *Journal of Hydrology, 296*, 1-22.
573
574 Masek, J.G. (2001). Stability of boreal forest stands during recent climate change:
575 evidence from Landsat satellite imagery. *Journal of Biogeography, 28*, 967-976.
576
577 McMahon, G., Wiken, E.B., & Gauthier, D.A. (2004). Toward a scientifically rigorous
578 basis for developing mapped ecological regions. *Environmental Management, 34,* S111-
579 S124.
580
581 Montesano, P.M., Nelson, R., Sun, G., Margolis, H., Kerber, A., & Ranson, K.J. (2009).
582 MODIS tree cover validation for the circumpolar taiga-tundra transition zone. *Remote*
583 *Sensing of Environment*. 113, 2130-2141.
584
585 Olson, D.M., Dinerstein, E., Wikramanayake, E.D., Burgess, N.D., Powell, G.V.N.,
586 Underwood, E.C., D'Amico, J.A., Itoua, I., Strand, H.E., Morrison, J.C., Loucks, C.J.,
587 Allnutt, T.F., Ricketts, T.H., Kura, Y., Lamoreux, J.F., Wettengel, W.W., Hedao, P., &
588 Kassem, K.R. (2001). Terrestrial ecoregions of the worlds: A new map of life on
589 Earth. *Bioscience, 51,* 933-938.
590
591 Olthof, I., Pouliot, D., Latifovic, R., & Chen, W.J. (2008). Recent (1986-2006)

592 Vegetation-Specific NDVI Trends in Northern Canada from Satellite Data. *Arctic, 61*,
593 381-394.
594
595 Osterkamp, T.E., & Romanovsky, V.E. (1996). Characteristics of changing permafrost
596 temperatures in the Alaskan Arctic, USA. *Arctic and Alpine Research*. 28(3), 267-273.
597
598 Osterkamp, T.E., & Jorgenson, J.C. (2006). Warming of permafrost in the Arctic
599 National Wildlife Refuge, Alaska. *Permafrost and Periglacial Processes, 17,* 65-69.
600
601 Pavlov, A.V. (1994). Current changes of climate and permafrost in the arctic and sub-
602 arctic of Russia. *Permafrost and Periglacial Processes.* 5(2), 101-110.
603
604 Payette, S., Fortin, M.J., & Gamache, I. (2001). The subarctic forest-tundra: the structure
605 of a biome in a changing climate. *Bioscience.* 51(9), 709-718.
606
607 Payette, S. & Gagnon, R. (1985). Late Holocene deforestation and tree regeneration in
608 the forest-tundra of Quebec. *Nature*, 313, 570-572.
609
610 Pekkarinen, A. (2002). A method for the segmentation of very high spatial resolution
611 images of forested landscapes. *International Journal of Remote Sensing, 23,* 2817-2836.
612
613 Potapov, P., Yaroshenko, A., Turubanova, S., Dubinin, M., Laestadius, L., C. Thies, D.
614 Aksenov, A. Egorov, Y. Yesipova, I. Glushkov, M. Karpachevskiy, A. Kostikova, A.
615 Manisha, E. Tsybikova, and I. Zhuravleva. (2008). Mapping the world's intact forest
616 landscapes by remote sensing. *Ecology and Society*, 13(2), 51. URL:
617 http://www.ecologyandsociety.org/vol13/iss2/art51/
618
619 Ranson, K.J., Sun, G., Kharuk, V.I., & Kovacs, K. (2004). Assessing tundra-taiga
620 boundary with multi-sensor satellite data. *Remote Sensing of Environment, 93,* 283-295.
621
622 Rees, G., Brown, I., Mikkola, K., Virtanen, T., & Werkman, B. (2002). How can the
623 dynamics of the tundra-taiga boundary be remotely monitored? *Ambio,* 56-62.
624
625 Serreze, M.C., Walsh, J.E., Chapin III, F.S., Osterkamp, T., Dyurgerov, M.,
626 Romanovsky, V., Oechel, W.C., Morison, J., Zhang, T. & Barry, R.G. (2000).
627 Observational evidence of recent change in the northern high-latitude environment.
628 *Climate Change*, 46, 159-207.
629
630 Skre, O., Baxter, R., Crawford, R.M.M., Callaghan, T.V., & Fedorkov, A. (2002). How
631 will the tundra-taiga interface respond to climate change? *Ambio,* 12,37-46.
632
633 Stow, D.A., Hope, A., McGuire, D., Verbyla, D., Gamon, J., Huemmrich, F., Houston,
634 S., Racine, C., Sturm, M., Tape, K., Hinzman, L., Yoshikawa, K., Tweedie, C., Noyle,
635 B., Silapaswan, C., Douglas, D., Griffith, B., Jia, G., Epstein, H., Walker, D., Daeschner,
636 S., Petersen, A., Zhou, L.M., & Myneni, R. (2004). Remote sensing of vegetation and
637 land-cover change in Arctic Tundra Ecosystems. *Remote Sensing of Environment, 89,*

281-308.

Swann, A.L., Fung, I.Y., Levis, S., Bonan, G.B., & Doney, S.C. (2010). Changes in Arctic vegetation amplify high-latitude warming through the greenhouse effect. *Proceedings of the National Academy of Sciences*, 107(4), 1295-1300.

Sun, G., Ranson, K.J., Kharuk, V.I., & Kovacs, K. (2004). Changes in the taiga-tundra boundary observed with Landsat. International Geoscience and Remote Sensing Symposium Proceedings, *2004 IEEE International* 2 (2004), 722–724.

Tape, K., Sturm, M., & Racine, C. (2006). The evidence for shrub expansion in Northern Alaska and the Pan-Arctic. *Global Change Biology*, 12, 686-702.

Tilton, J., Lawrence, W.T., & Plaza, A.J. (2006). Utilizing hierarchical segmentation to generate water and snow masks to facilitate monitoring change with remotely sensed image data. *GIScience & Remote Sensing*, 2006, 43(1), 39-66.

Timoney, K.P., La Roi, G.H., Zoltai, S.C., & Robinson, A.L. (1992). The high subarctic forest-tundra of northwestern Canada: Position, Width, and Vegetation Gradients in relation to climate. *Arctic*, 45(1), 1-9.

Timoney, K.P. (1995). Tree and tundra cover anomalies in the sub-arctic forest-tundra and northwestern Canada. *Arctic*, 48(1), 13-21.

Toutoubalina, O.V., & Rees, W.G. (1999). Remote sensing of industrial impact on Arctic vegetation around Noril'sk, northern Siberia: preliminary results. *International Journal of Remote Sensing, 20*, 2979-2990.

van Aardt, J.A.N., Wynne, R.H., & Oderwald, R.G. (2006). Forest volume and biomass estimation using small-footprint lidar-distributional parameters on a per-segment basis. *Forest Science, 52*, 636-649.

Verbyla, D. (2008). The greening and browning of Alaska based on 1982-2003 satellite data. *Global Ecology and Biogeography, 17*, 547-555.

Virtanen, T., Mikkola, K., Patova, E., & Nikula, A. (2002). Satellite image analysis of human caused changes in the tundra vegetation around the city of Vorkuta, north-European Russia. *Environmental Pollution, 120*, 647-658.

Vlassova, T.K. (2002). Human impacts on the tundra-taiga zone dynamics: The case of the Russian lesotundra. *Ambio*, 30-36.

Walker, D.A., Raynolds, M.K., Daniels, F.J.A., Einarsson, E., Elvebakk, A., Gould, W.A., Katenin, A.E., Kholod, S.S., Markon, C.J., Melnikov, E.S., Moskalenko, N.G., Talbot, S.S., Yurtsev, B.A., & Team, C. (2005). The Circumpolar Arctic vegetation map. *Journal of Vegetation Science, 16*, 267-282.

Walker M.D., Wahren C.H., Hollister R.D. et al. (2006). Plant community responses to experimental warming across the tundra biome. Proceedings of the National Academy of Sciences, 103, 1342–1346.

Wulder, M.A., White, J.C., Cranny, M., Hall, R.J., Luther, J.E., Beaudoin, A., Goodenough, D.G., & Dechka, J.A. (2008). Monitoring Canada's forests. Part 1: completion of the EOSD land cover project. *Canadian Journal of Remote Sensing.* 34(6), 549-562.

Tables

Table 1. Slope and y-intercept values of the linear adjustments for each circumpolar zone. Longitudes shown are the western and eastern bounds of each zone. Slope and y-intercept values based on results from Montesano et al. 2009.

	Longitudinal Bounds			
Name	West	East	Slope	y - intercept
Alaska	-180	-130	0.54	18.6
Western / Cent. Canada	-130	-80	0.53	24.58
Eastern Canada	-80	-55	0.66	10.96
Scandinavia	4	40	0.27	21.83
Western Eurasia	40	60	0.47	24.91
Central Eurasia	60	110	0.54	13.51
Eastern Eurasia	110	180	0.41	18.37

Table 2. Summary of the intersection of VCF_{adj} with CAVM and CAPI tree-lines. Regional longitudinal zone means are aggregated from 1° longitudinal zone means.

	Mean %TCC of 1° long. zones		Proportion of 1° zones with <5% mean %TCC	
Name	CAVM	CAPI	CAVM	CAPI
Alaska	7.3	8.1	0.43	0.46
Western / Cent. Canada	0.5	0.5	1.00	0.97
Eastern Canada	3.0	6.3	0.69	0.56
Scandinavia	---	6.2	---	0.60
Western Eurasia	23.0	7.9	0.00	0.45
Central Eurasia	10.9	11.8	0.45	0.37
Eastern Eurasia	6.7	6.2	0.63	0.58

Table 3. Area of both circumpolar ecotone classes broken down by regional zone. TTE Class 1 includes polygons with tree canopy cover of 5%-20%. TTE Class 2 includes polygons with <5% mean tree canopy cover and with a standard deviation of >5% mean tree canopy cover.

	Area (sq. km.)		
Name	TTE Class 1	TTE Class 2	Ratio: TTE Class 1 / TTE Class 2
Alaska	183,846	83,307	2.2
Western / Cent. Canada	305,032	35,756	8.5
Eastern Canada	123,155	35,172	3.5
Scandinavia	49,029	35,333	1.4
Western Eurasia	53,389	32,694	1.6
Central Eurasia	269,404	119,007	2.3
Eastern Eurasia	322,080	300,842	1.1

Figures

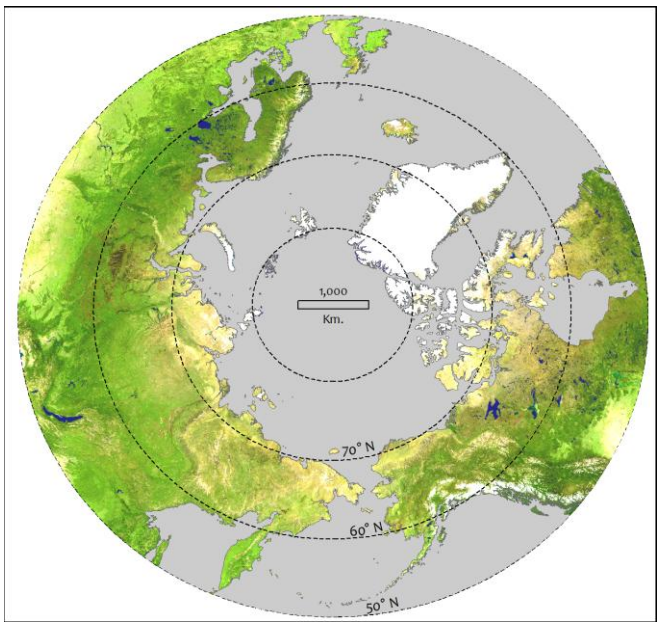

Figure 1. MODIS cloud free composite of the northern hemisphere in summer. The circumpolar taiga-tundra ecotone benchmarked in this study is about 13400km long. Image source: earthobservatory.nasa.gov

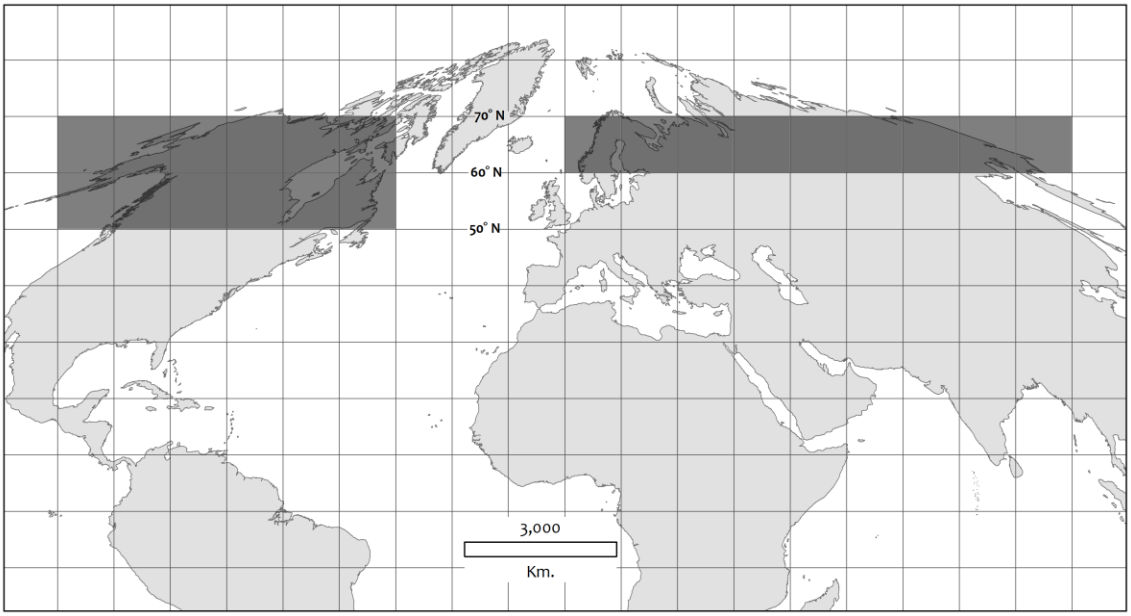

Figure 2. The 21 Collection 4 MODIS VCF tiles gathered for continental North America and Eurasia. Each tile is 10° X 10 ° and gridded in the sinusoidal projection.

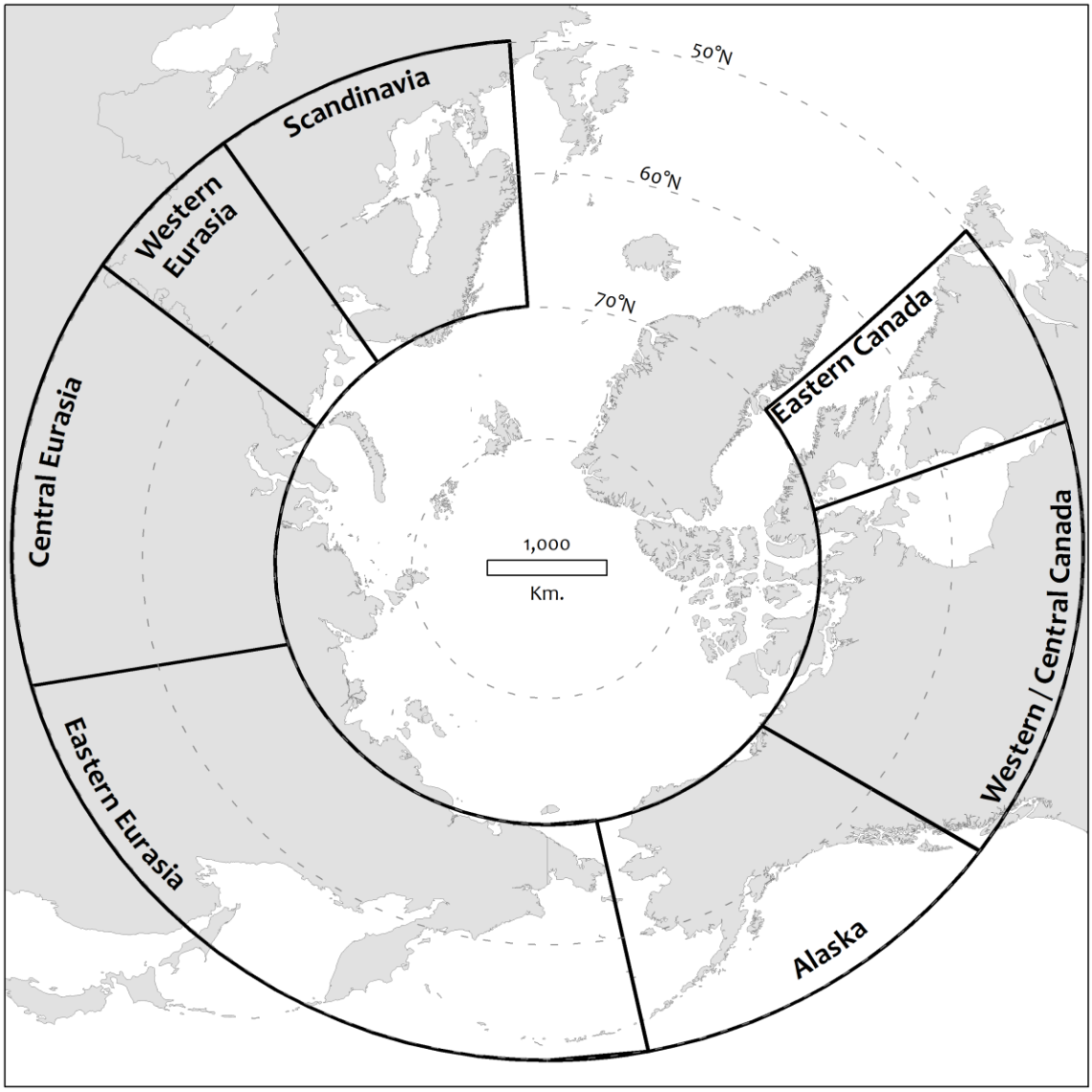

Figure 3. The 7 circumpolar zones by which linear equations adjusting VCF tree canopy cover values were applied.

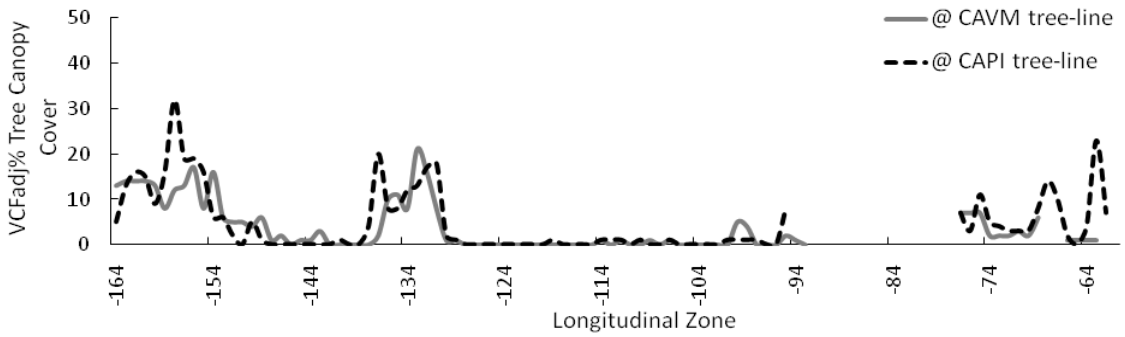

Figure 4a Mean VCF_{adj} values in each 1° longitudinal zone at the intersection with CAVM and CAPI tree lines in North America.

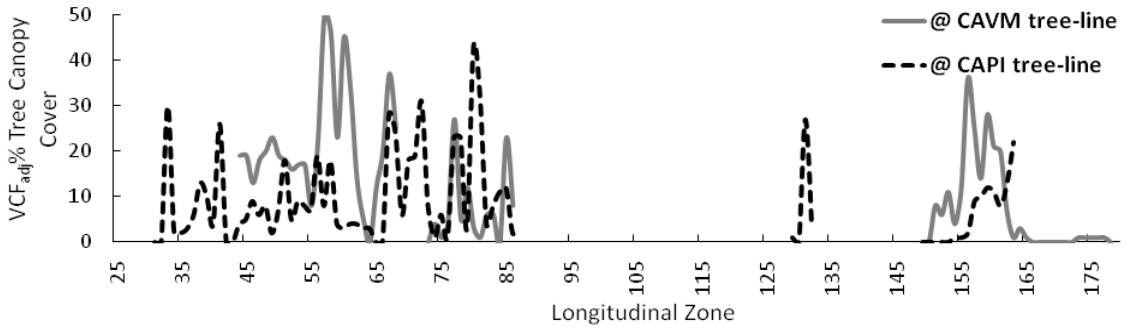

Figure 4b Mean VCF_{adj} values in each 1° longitudinal zone at the intersection with CAVM and CAPI tree lines in Eurasia.

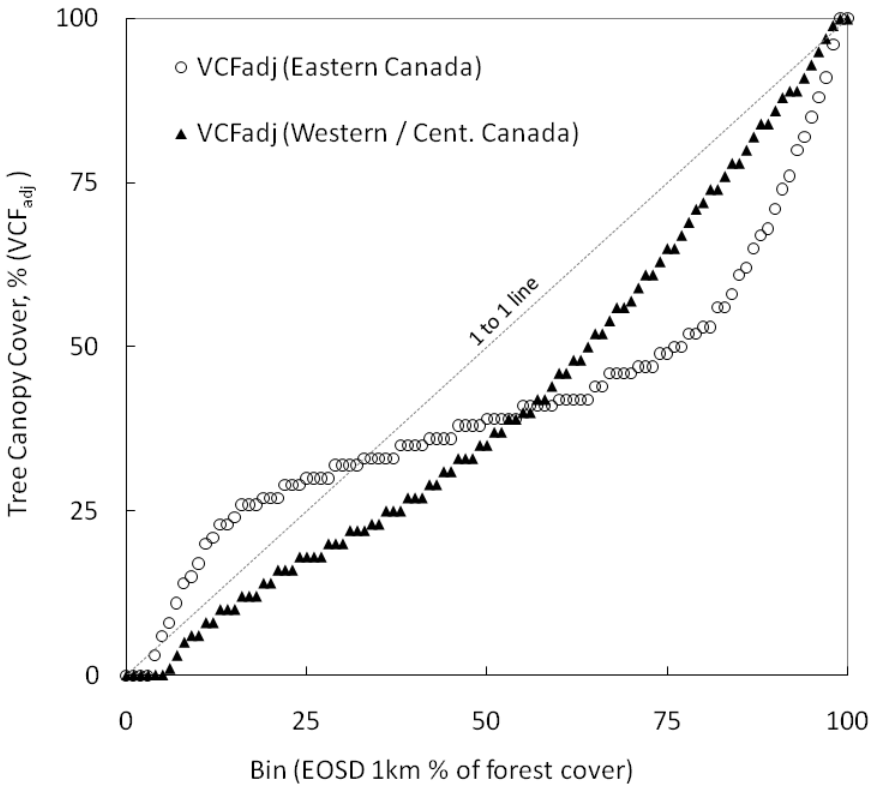

Figure 5. The median value of VCF_{adj} %TCC for each bin of EOSD proportion of forest at 1% intervals.

Figure 6. The circumpolar taiga-tundra ecotone (TTE) map (6a). TTE Class 1 (red) depicts areas with a mean of 5-20% tree canopy cover and TTE Class 2 (blue) depicts areas of tree canopy cover <5% and standard deviation >5%. Dark green areas identify the boreal forest ecozone, light green areas are nonforest/ice/rock/tundra, and grey areas are those above 70 degrees N (no Collection 4 MODIS VCF data) or below 60 degrees (Eastern Hemsiphere) or 50 degrees (Western Hemisphere). Figures 6 b-g depict larger scale versions of the 6a map, beginning in Alaska and moving to the east.

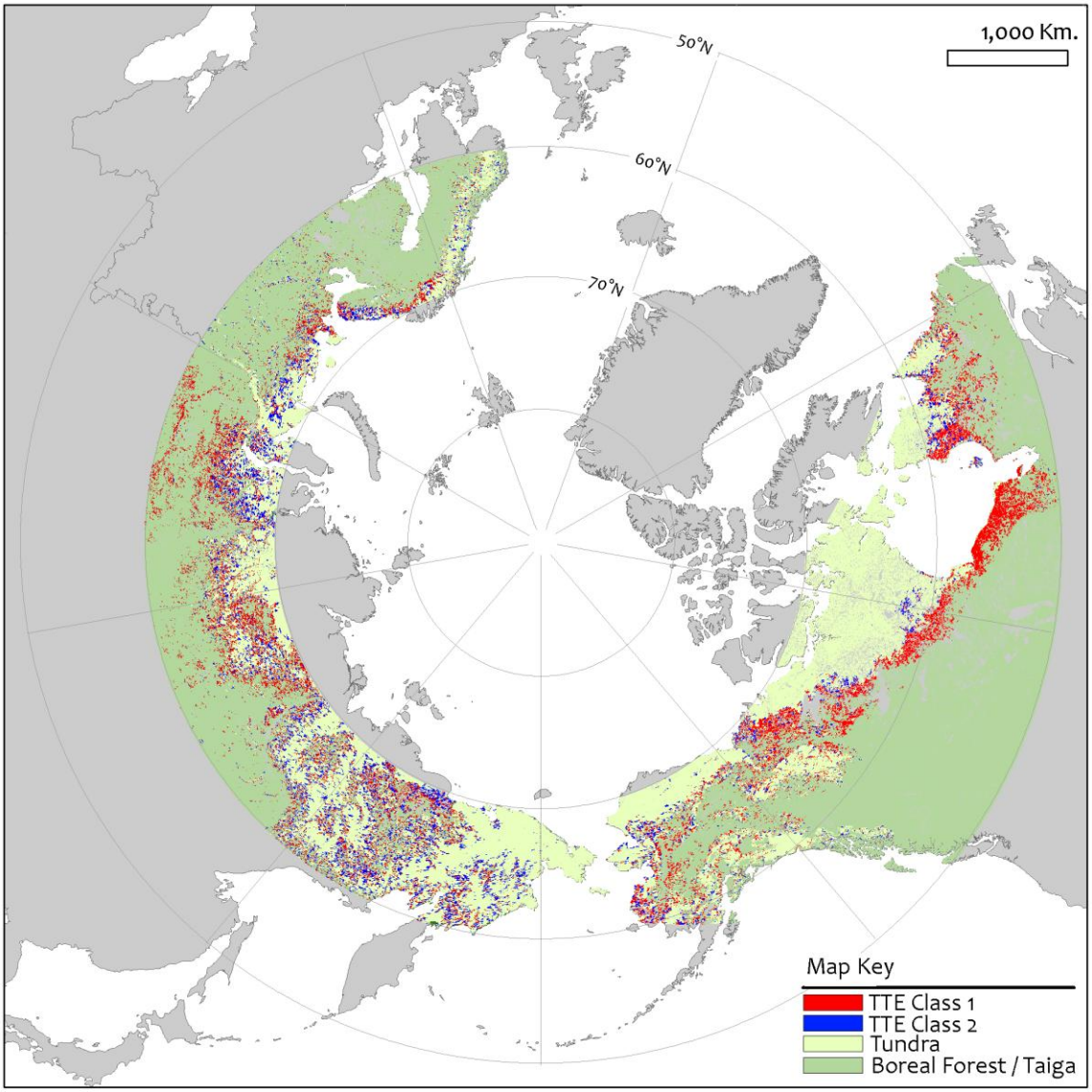
1,000 Km.
50°N
60°N
70°N
Map Key
TTE Class 1
TTE Class 2
Tundra
Boreal Forest / Taiga

Figure 6a

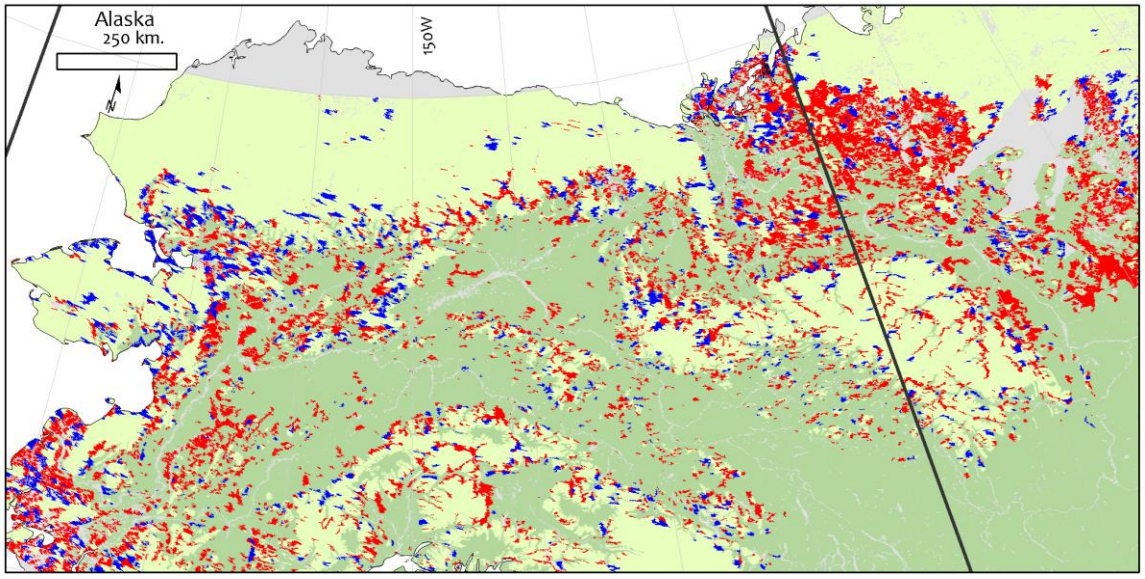

Figure 6b

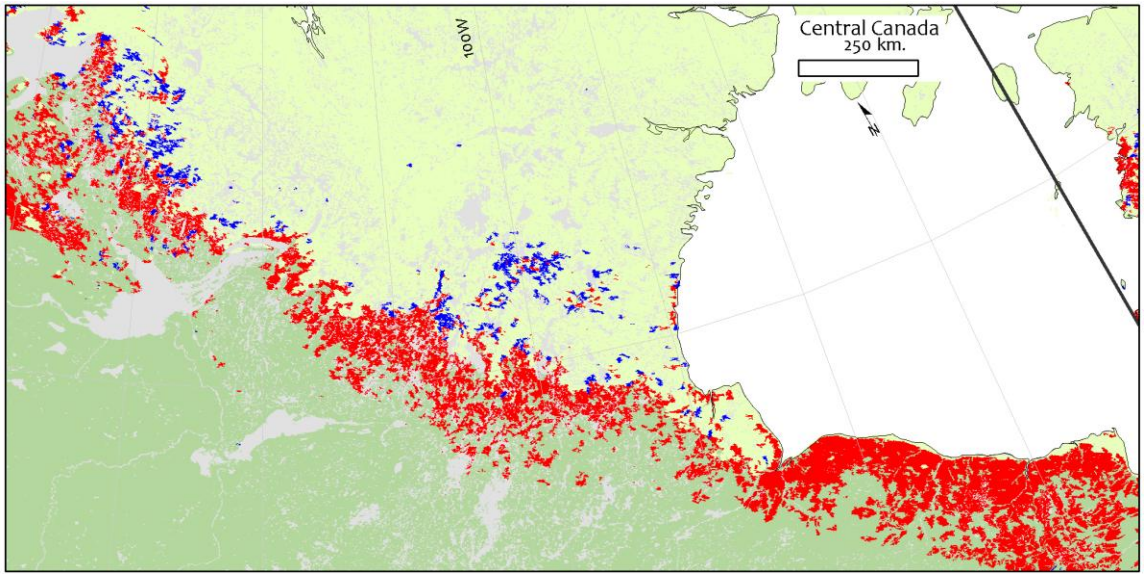

Figure 6c

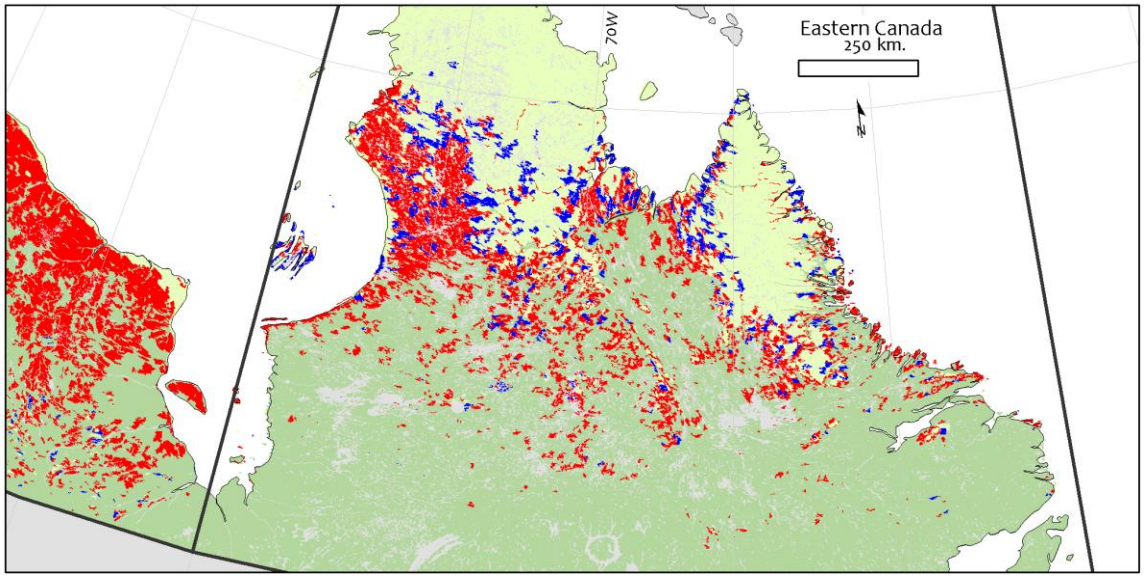

Figure 6d

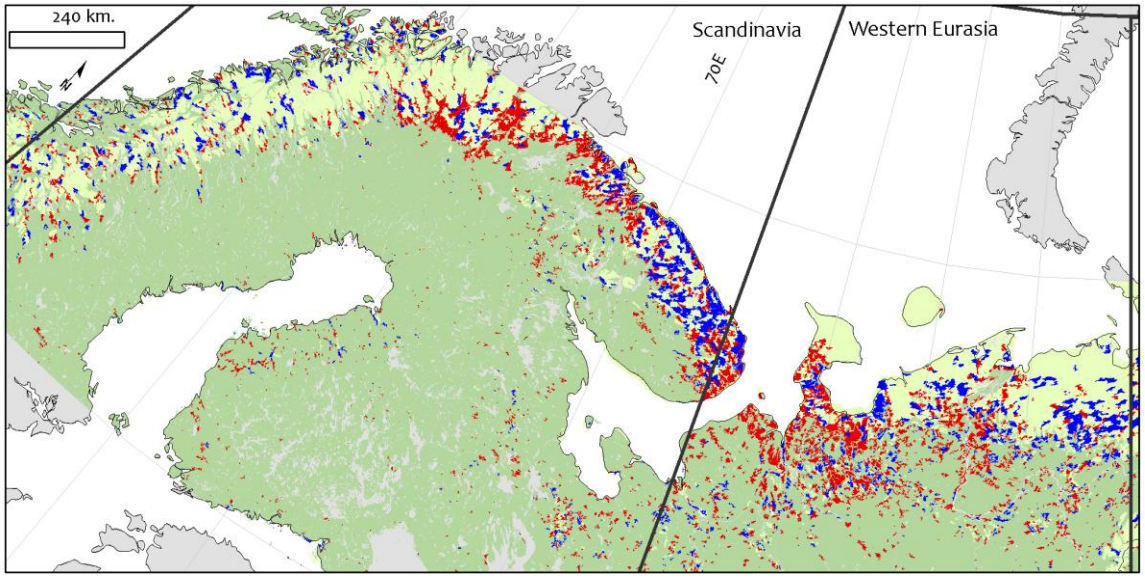

Figure 6e

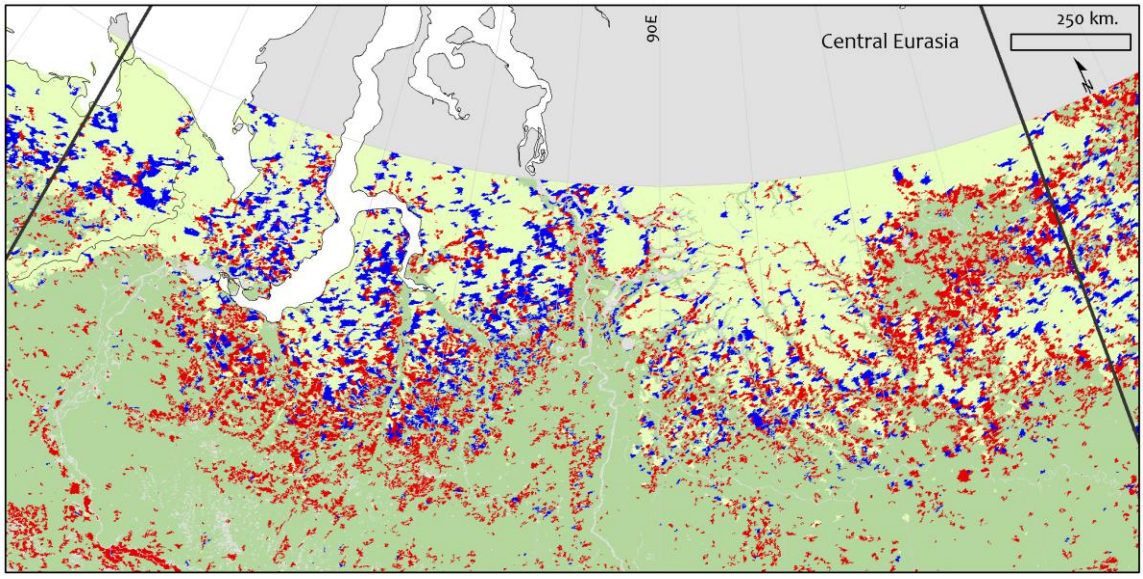

Figure 6f

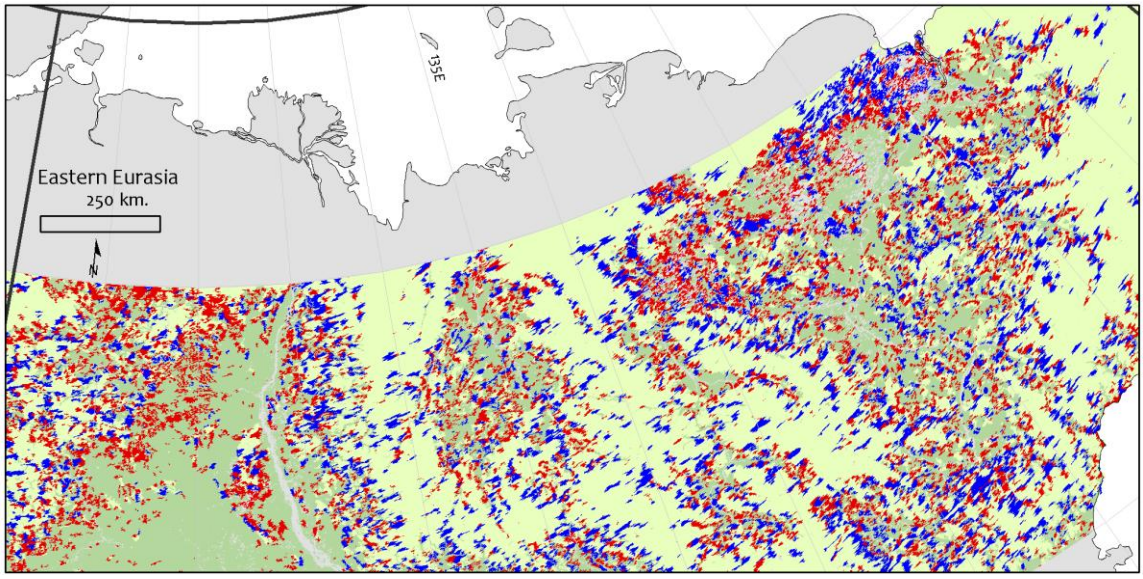

Figure 6g